Identification of Tensin-3 as a MALT1 substrate that controls B cell adhesion and lymphoma dissemination

Mélanie Juilland[a,1] (ID), Nagham Alouche[a,1], Ivana Ubezzi[a,1,2], Montserrat Gonzalez[a], Harun-Or Rashid[a] (ID), Leonardo Scarpellino[a], Tabea Erdmann[b], Michael Grau[b] (ID), Georg Lenz[b], Sanjiv A. Luther[a] (ID), and Margot Thome[a,3] (ID)

The protease MALT1 promotes lymphocyte activation and lymphomagenesis by cleaving a limited set of cellular substrates, most of which control gene expression. Here, we identified the integrin-binding scaffold protein Tensin-3 as a MALT1 substrate in activated human B cells. Activated B cells lacking Tensin-3 showed decreased integrin-dependent adhesion but exhibited comparable NF-κB1 and Jun N-terminal kinase transcriptional responses. Cells expressing a noncleavable form of Tensin-3, on the other hand, showed increased adhesion. To test the role of Tensin-3 cleavage in vivo, mice expressing a noncleavable version of Tensin-3 were generated, which showed a partial reduction in the T cell–dependent B cell response. Interestingly, human diffuse large B cell lymphomas and mantle cell lymphomas with constitutive MALT1 activity showed strong constitutive Tensin-3 cleavage and a decrease in uncleaved Tensin-3 levels. Moreover, silencing of Tensin-3 expression in MALT1-driven lymphoma promoted dissemination of xenografted lymphoma cells to the bone marrow and spleen. Thus, MALT1-dependent Tensin-3 cleavage reveals a unique aspect of the function of MALT1, which negatively regulates integrin-dependent B cell adhesion and facilitates metastatic spread of B cell lymphomas.

paracaspase | DLBCL | integrin | metastasis

The arginine-specific cysteine protease MALT1 (also known as paracaspase) has recently emerged as a signaling protein that contributes to several aspects of lymphocyte activation and the development of marginal zone (MZ) B cells, B1 B cells, and regulatory T (Treg) cells (1, 2). The protease activity of MALT1 accounts to a large part for its capacity to promote proper lymphocyte activation and development (3–6), but the contribution of individual MALT1 substrates to the observed phenotypes remains largely unexplored.

Upon antigen receptor engagement, MALT1 is activated as a consequence of the formation of a multimeric CARMA1-BCL10-MALT1 complex that is thought to favor MALT1-dependent recruitment of additional signaling proteins and to unleash the protease activity of MALT1 by means of MALT1's inducible oligomerization and monoubiquitination (7–11). Once activated, MALT1 controls various aspects of lymphocyte activation and differentiation, mainly through the regulation of gene transcription (1, 2). As a scaffold, MALT1 promotes the activation of the transcription factor NF-κB1 by recruiting the ubiquitin ligase TRAF6, which favors the activation of the IκB kinase complex and leads to the phosphorylation-dependent degradation of the NF-κB1 inhibitor IκB by the proteasome (7, 12). The protease activity of MALT1, on the other hand, facilitates activation of the transcription factors NF-κB1 and AP-1 through cleavage of additional proteins with inhibitory functions, including the deubiquitinating enzymes A20 and CYLD (13), the NF-κB family member RelB (14), and by autoprocessing of MALT1 (15). As a protease, MALT1 additionally controls gene expression by cleaving negative regulators of mRNA stability, including the RNAses Regnase-1 (also known as MCPIP-1 or ZC3H12a) (16) and N4BP-1 (17) and the posttranscriptional repressor proteins Roquin-1 and -2 (18). Additional MALT1 substrates that modulate transcriptional responses of lymphocytes include the linear ubiquitination assembly complex component heme-oxidized IRP2 Ub ligase 1 (HOIL-1) (19–21) and likely a variety of additional proteins whose contributions are less well understood (22).

A limited number of MALT1 substrates have been identified that exert transcription-independent functions, linked to the regulation of the cytoskeleton and cell adhesion. These include BCL10, whose cleavage controls T cell adhesion (23), the tumor suppressor LIMA1, whose cleavage supports proliferation and adhesion of B cells (24), and CYLD, which in addition to promoting AP-1-dependent transcription favors the disassembly of microtubules and induces changes in endothelial cell permeability (25).

In the present study, we identified Tensin-3 as a MALT1 substrate. Tensins form a family of 4 structurally related proteins encoded by separate genes. Tensin-1, -2, and -3 are thought to regulate the adhesion and migration of epithelial cells, by forming a physical link between the actin cytoskeleton and the cytoplasmic portion of certain beta integrin chains (26, 27).

Significance

By cleaving a variety of cytoplasmic signaling proteins, the protease MALT1 promotes adaptive immunity and lymphoma development. The regulation of gene transcription is a major outcome of MALT1-dependent substrate cleavage, but transcription-independent activities of MALT1 substrates have started to emerge. Here, we found that Tensin-3, a recognized regulator of integrin-dependent epithelial cell adhesion, is cleaved by MALT1, limiting the adhesion of activated B cells and human B cell lymphoma lines. In vivo, Tensin-3 cleavage was required for optimal germinal center B cell responses, and low Tensin-3 levels promoted metastatic lymphoma dissemination. These findings identify a unique, transcription-independent role of MALT1 in the control of cellular adhesiveness, which is relevant for its proto-oncogene function.

Binding of these Tensins to actin is mediated by an N-terminal actin-binding domain (ABD) that is lacking in the shorter protein Tensin-4 (also known as CTEN) (26). The C-terminal (CT) region of all 4 Tensin proteins contains a Src homology-2 (SH2) and a phosphotyrosine-binding (PTB) domain that is thought to interact with NPxY motifs in the cytoplasmic tails of certain integrin beta chains (28, 29). The sequence between the ABD and the SH2 domain is unique to each Tensin family member, suggesting additional, exclusive physiological functions.

Here, the identification and characterization of Tensin-3 as a MALT1 substrate is reported along with its role as negative regulator of integrin-dependent B cell adhesion, which affects the function of normal and transformed B cells.

Results

MALT1 Cleaves the Tensin Family Member, Tensin-3. We and others have previously shown that MALT1 is constitutively active in cell lines derived from the activated B-cell (ABC) subtype of diffuse large B-cell lymphomas (DLBCL) (30, 31). We therefore reasoned that inhibition of MALT1 protease activity should result in accumulation of uncleaved MALT1 substrates in these cells and allow the identification of unknown MALT1 substrates by a mass spectrometry (MS)-based approach. To this end, we treated the ABC DLBCL cell line OCI-Ly3 with the MALT1 tetrapeptide inhibitor z-LVSR-fmk (15) for 16 h and compared total protein levels in treated vs. untreated cells, as a function of molecular weight, using a SILAC-based quantitative MS approach (Fig. 1A). Inhibitor treatment led to accumulation of a variety of potential MALT1 substrates (the full list of the candidates and corresponding legends are depicted in Datasets S1 and S2, the details for each gel slice and the corresponding legends are depicted in Datasets S3 and S4). Among these, we observed a 3.7-fold increase in the levels of the full-length form of the previously identified MALT1 substrate RelB (14), validating our approach (Fig. 1 B and C). Interestingly, inhibitor treatment also revealed a 5.2-fold accumulation of the protein Tensin-3 (Fig. 1 B and C). A second analysis was performed, to sort on proteins that showed at
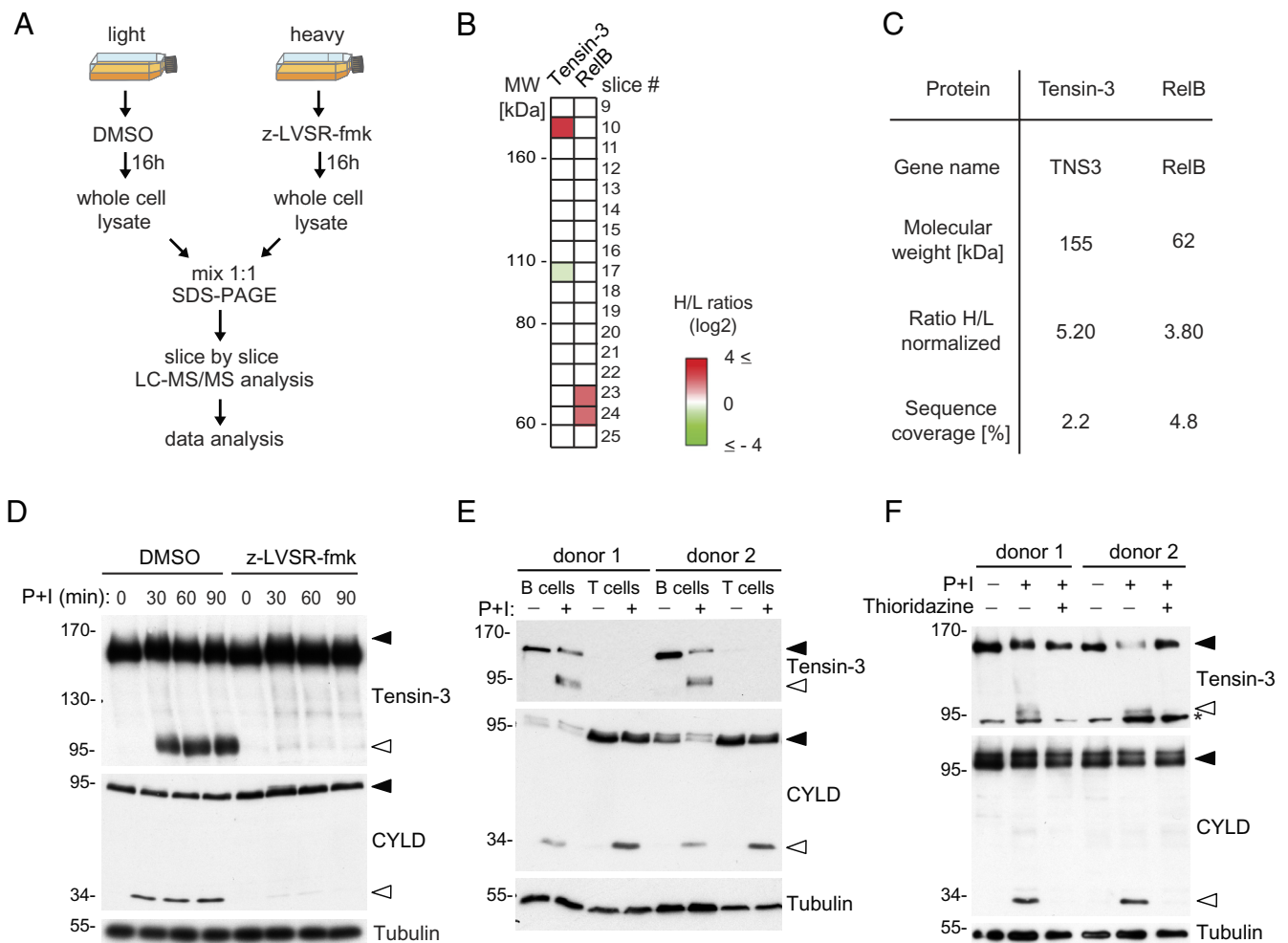

Fig. 1. Tensin-3 is a MALT1 substrate in activated human B cells. (A) OCI-Ly3 cells grown in medium with "light" or "heavy" isotope-containing amino acids were treated with z-LVSR-fmk or solvent (dimethyl sulfoxide, DMSO) for 16 h. Cell lysates were mixed, run on SDS-PAGE and the gel was cut into 51 slices. Each slice was analysed individually by tryptic digestion and liquid chromatography/tandem MS (LC–MS/MS). (B) MS results for Tensin-3 and RelB. Color code indicates the z-LVSR-fmk-induced change in the ratio between heavy/light proteins in the indicated gel slice. (C) Table showing changes of Tensin-3 and RelB expression levels in HBL-1 cells upon treatment with z-LVSR-fmk for 16 h (H, heavy isotope labelled), relative to solvent treated (L, light isotope labelled) cells. (D) Western blot analysis of BJAB cells, pretreated with z-LVSR-fmk or solvent alone (DMSO) and stimulated for the indicated times with PMA and ionomycin (P+I). (E and F) Immunoblot analysis of Tensin-3 cleavage in lysates of human primary CD19+ B and CD4+ T cells (E) or human primary CD19+ B cells (F), isolated from two independent healthy donors. Cells were incubated with or without PMA and ionomycin (P+I) for 30 min (E and F) and pretreated with thioridazine or solvent alone for 1 h before stimulation (F). Blotting for CYLD was used to monitor MALT1 activity. Black and open arrowheads indicate noncleaved and cleaved forms, respectively, of Tensin-3 or CYLD. Tubulin serves as loading control throughout, and an asterisk indicates a nonspecific band. Positions of molecular weight markers are indicated in kDa. Data are representative of one (B and C) or two independent experiments (D), or a single experiment, each performed with cells from two independent donors (E and F).

least a 1.41-fold increase and a corresponding 1.41-fold decrease in a higher and a lower MW gel slice, respectively (209 proteins that matched these criteria, and the corresponding legends are listed in Datasets S5 and S6). Tensin-3 was further validated as a possible MALT1 substrate by this analysis.

Next, we assessed whether Tensin-3 cleavage could indeed be induced by MALT1 activation in human B cell lines and primary B cells. In the GCB (germinal center B cell) DLBCL cell line BJAB, Tensin-3 cleavage could be induced upon stimulation with the phorbolester phorbol-12-myristate-13-acetate (PMA) and the calcium ionophore ionomycin, which lead to activation of PKC family members and thereby mimic several aspects of BCR signaling (Fig. 1D). The observed cleavage of Tensin-3, but also of another MALT1 substrate, CYLD, was efficiently inhibited by pretreatment of the cells with z-LVSR-fmk. We subsequently explored Tensin-3 expression and cleavage in primary human lymphocytes. Tensin-3 was well expressed in human primary B cells isolated from independent donors, while its levels were low to undetectable in the corresponding T cell preparations (Fig. 1E). This contrasts with the expression of CYLD, which was well expressed in T cells and, weaker, in B cells (Fig. 1E). Tensin-3 levels were also very low or undetectable in various T cell lines, including Jurkat, Hut78, and MOLT4 (not depicted). Stimulation of the primary human B cells using PMA and ionomycin led to a highly efficient induction of Tensin-3 cleavage, which was blocked upon preincubation of the cells with the allosteric MALT1 inhibitor thioridazine (32) (Fig. 1F). Collectively, these findings identify Tensin-3 as a substrate of MALT1 in activated B cells.

MALT1 Cleaves Human and Mouse Tensin-3 after Two Conserved Arg Residues. To identify the MALT1-dependent cleavage site(s) in Tensin-3, we assessed its cleavage in 293T cells. In these, MALT1 can be activated by its coexpression with BCL10 (which expresses as multiple phosphorylation isoforms in this setting) (13, 23). Under these conditions, we observed formation of doublets of NT (N-terminal) and CT Tensin-3 fragments of approximately 72 kDa and 95 kDa, respectively (Fig. 2A), which is consistent with the cleavage pattern observed for endogenous Tensin-3 (Fig. 1). Cleavage was strongly impaired upon treatment of cells with the MALT1 inhibitor z-LVSR-fmk, leading to accumulation of full-length Tensin-3 in presence of MALT1 and BCL10 (Fig. 2A). To confirm the requirement of MALT1 protease activity, we also expressed Tensin-3 together with wild-type (wt) or catalytically inactive MALT1 (MALT1 C464A) in 293T cells. Coexpression of Tensin-3 with wt MALT1 induced Tensin-3 cleavage, while MALT1 C464A was not able to cleave Tensin-3 (Fig. 2B). Interestingly, the sole coexpression of Tensin-3 with MALT1 was sufficient to induce Tensin-3 cleavage, in contrast to other substrates such as RelB, A20, CYLD, or Regnase-1 that need coexpression of BCL10 together with MALT1 to induce their cleavage (13, 14, 16, 33).

Tensin-3 shares homology with Tensin-1, -2, and -4 (also known as CTEN) (Fig. 2C). Therefore, we verified whether other human Tensin proteins could be cleaved by MALT1. However, among the four family members, only Tensin-3 was cleaved by MALT1 (Fig. 2D). To identify the cleavage site(s) of Tensin-3, we mutated candidate arginine residues in sequence motifs that matched the described optimal cleavage motif, Φ-x-S/P-R, in which a hydrophobic (Φ) and a variable (x) amino acid precede a Ser or Pro residue that is followed by an Arg residue, after which cleavage occurs (34). Mutation of one such Arg residue, R614 within the sequence motif $LVSR_{614}$, strongly reduced MALT1-dependent cleavage of human Tensin-3 (hTensin-3) in 293T cells, but still allowed for residual cleavage to occur, which resulted in a CT fragment with slightly lower mobility in sodium dodecyl-sulfate polyacrylamide gel

electrophoresis (SDS-PAGE) (Fig. 2E). Mutation of R645 within the sequence motif $AVQR_{645}$ partially reduced Tensin-3 cleavage, whereas mutation of both, R614 and R645, fully prevented cleavage (Fig. 2E). Thus, MALT1 cleaves hTensin-3 after R614 and R645 within its structurally undefined linker region (Fig. 2F).

To assess whether these sites correspond to natural Tensin-3 cleavage sites in ABCs, we overexpressed wt Tensin-3 or its R614G/R645G double mutant in BJAB cells that were silenced for endogenous Tensin-3 expression. Stimulation of these cells with PMA and ionomycin induced cleavage of wt but not of the R614G/R645G double mutant form of hTensin-3 (Fig. 2G). Interestingly, these two residues are conserved in the mouse sequence and their mutation similarly prevented cleavage of mouse Tensin-3 (mTensin-3) upon coexpression with MALT1 and BCL10 in 293T cells (Fig. 2H). Thus, MALT1 cleaves hTensin-3 and mTensin-3 after R614 and R645.

The activation of MALT1 in B cells depends on the scaffold protein CARMA1 (also known as CARD11), while MALT1 activation in other inflammatory contexts relies on the CARMA1 homologs CARMA2 (CARD14), CARMA3 (CARD10), and CARD9 (1, 2, 35). To determine whether CARD proteins other than CARMA1 can induce Tensin-3 cleavage, Tensin-3 or its noncleavable R614G/R645G mutant were coexpressed with CARMA1, CARMA2, CARMA3, or CARD9 in 293T cells. Coexpression with CARMA1 induced cleavage of wt, but not of mutant Tensin-3. In contrast, CARMA2, CARMA3, and CARD9 were unable to induce Tensin-3 cleavage (SI Appendix, Fig. S1A). However, all CARD proteins induced cleavage of the MALT1 substrate CYLD under similar conditions (SI Appendix, Fig. S1B). Collectively, these findings identify Tensin-3 as a MALT1 substrate whose cleavage seems to specifically depend on a CARMA1-induced signaling event.

Mice Expressing a Noncleavable Form of Tensin-3 Show Partially Reduced B Cell Immune Responses. Based on our in vitro studies, we hypothesized that Tensin-3 cleavage might affect the development and/or function of B cells in vivo. Therefore, we generated mice expressing a noncleavable (nc), R614A/R645A double mutant form of Tensin-3 (subsequently named TNS3-nc mice) (Fig. 3A). Wt and TNS3-nc mice could be clearly distinguished by PCR-based genotyping (Fig. 3B) and presence of the point mutations was also verified by sequencing (SI Appendix, Fig. S2). With the presently available commercial anti-Tensin-3 antibodies, we were unable to reliably detect Tensin-3 protein expression in various murine lymphoid organs, but Tensin-3 mRNA levels were found to be comparable between wt and TNS3-nc mice (Fig. 3C). TNS3-nc mice were born in Mendelian ratios and showed no obvious signs of developmental abnormalities. Basal analysis of the mice revealed no significant differences between adult wt and TNS3-nc mice with respect to the absolute numbers and percentages of B and T cells in the spleen, lymph nodes, and the bone marrow (BM) (SI Appendix, Fig. S3 A–C). Similarly, the numbers and percentages of Treg cells in various organs (SI Appendix, Fig. S3D), as well as of follicular B cells within the spleen were unchanged (SI Appendix, Fig. S3E). Splenic MZ B cells and peritoneal B1a cells, which are absent or reduced in MALT1-deficient or -mutant mice (3–6, 36, 37), were also present in normal numbers and percentages (SI Appendix, Fig. S3 F and G).

Next, we tested proliferative responses of splenic B cells, isolated from naive wt and TNS3-nc mice, in response to in vitro stimulation with anti-IgM, PMA and ionomycin, or CpG. In all settings, B cell expansion was unaltered (SI Appendix, Fig. S4 A–C). Tensin-3 cleavage was also not required for the generation of the basal serum levels of IgM, IgG1 (Fig. 3D), and other antibody isotypes (SI Appendix, Fig. S4D), which were comparable in naive wt and TNS3-nc littermate mice. We next assessed whether
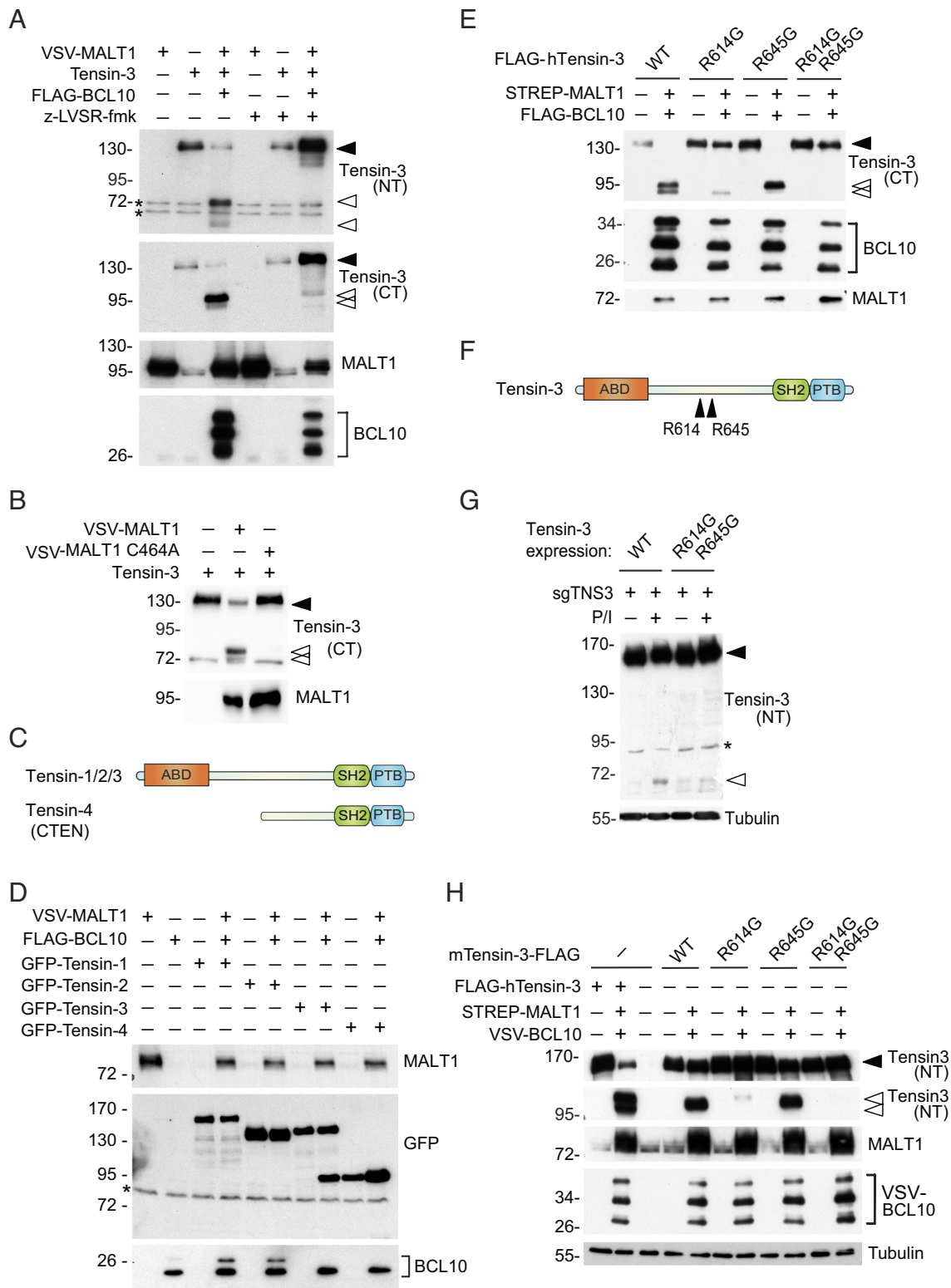
Fig. 2. MALT1 cleaves human and mouse Tensin-3 after R614 and R645. (*A*) Immunoblot analysis of 293T cells transfected with the indicated combinations of VSV-tagged MALT1, untagged Tensin-3 or FLAG-tagged BCL10, and given either no treatment (−) or treated for 16 h (+) with z-LVSR-fmk. Tensin-3 cleavage was assessed using antibodies directed against the NT or CT part of Tensin-3. (*B*) Immunoblot analysis of 293T cells transfected with the indicated combinations of VSV-tagged MALT1 or MALT1 C464 (a catalytically inactive mutant) and untagged Tensin-3. (*C*) Overview of the domain structure of Tensin family members. ABD: actin-binding domain; SH2: src homology domain 2; PTB: phosphotyrosine binding domain. (*D*) Immunoblot analysis of 293T cells transfected with the indicated combinations of GFP-tagged Tensin-1, -2, -3, and -4 (CTEN), VSV-tagged MALT1 and FLAG-tagged BCL10. (*E*) Immunoblot analysis of 293T cells transfected with the indicated combinations of STREP-tagged MALT1, FLAG-tagged human Tensin-3 (hTensin-3) or FLAG-tagged BCL10 constructs. (*F*) Overview of the domain structure of Tensin-3 and the position of the cleavage sites R614 and R645. ABD: actin-binding domain; SH2: src homology domain 2; PTB: phosphotyrosine binding domain. (*G*) Tensin-3-deficient BJAB cells were transduced with the indicated Tensin-3 constructs and incubated for 1 h with (+) or without (−) PMA and ionomycin (P+I). Tensin-3 cleavage was analysed by western blotting using an antibody directed against the NT part of Tensin-3. (*H*) Immunoblot analysis of 293T cells transfected with the indicated combinations of STREP-tagged MALT1, FLAG-tagged mouse Tensin-3 (mTensin-3), hTensin-3, or VSV-tagged BCL10 constructs. Black and open arrowheads indicate uncleaved and cleaved forms, respectively, of Tensin-3. Tubulin served as loading control, * indicates nonspecific bands. Data in all panels are representative of two independent experiments.
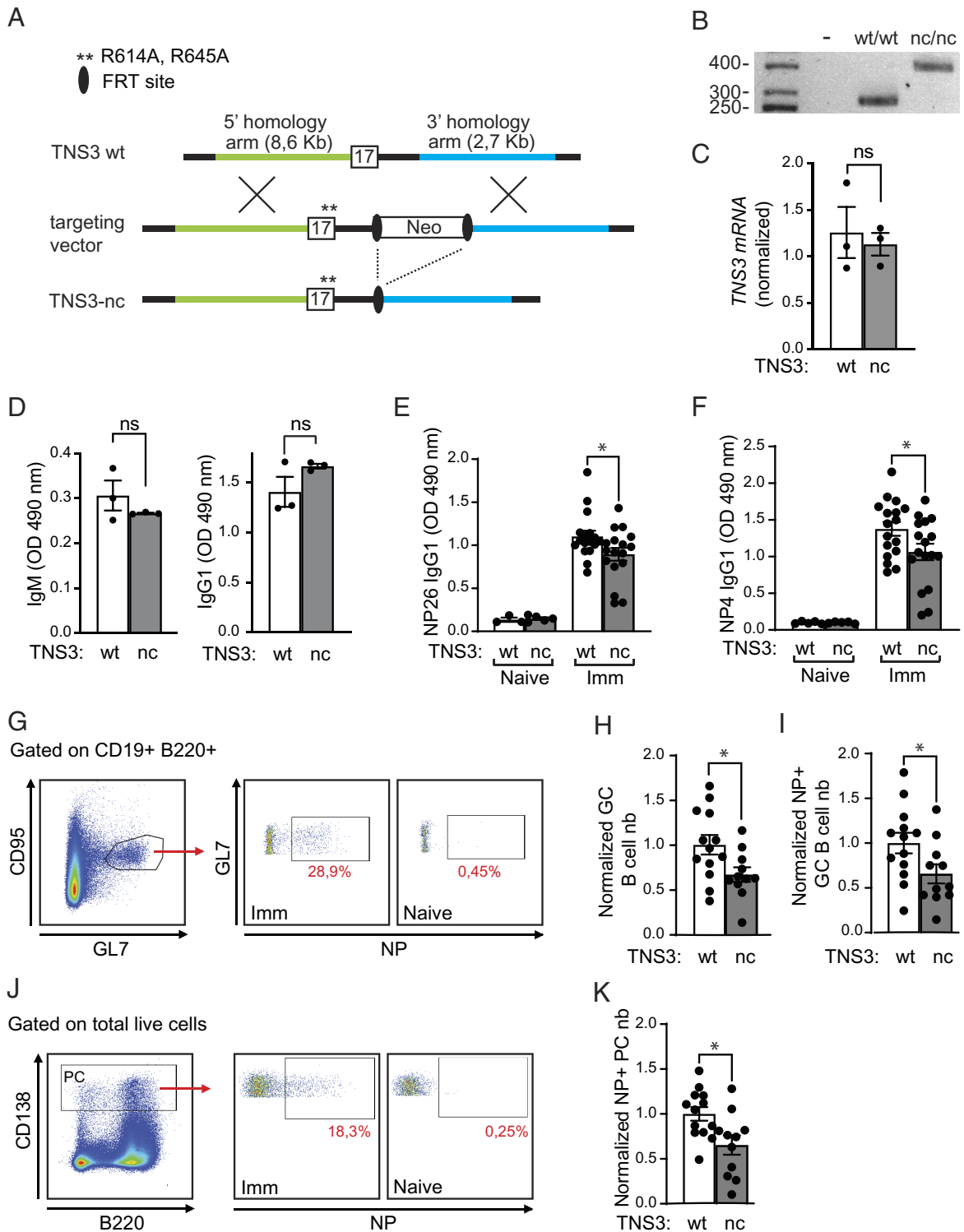
Fig. 3. Newly generated mice deficient in Tensin-3 cleavage show partially reduced B cell responses. (*A*) Overview of the targeting vector used to generate mice expressing noncleavable Tensin-3 (Tensin-3-nc). The vector carries two point mutations in exon 17, resulting in R614A and R645A point mutations, a neomycin resistance cassette (Neo) flanked by flippase recombinase target (FRT) sites along with the 5′ and 3′ homology arms. In the TNS3-nc mice used for this study, the Neo cassette was removed in a cross to mice expressing the flippase recombinase (FLP). (*B*) Genotyping of homozygous wild-type (wt/wt) and TNS3-nc (nc/nc) mice by PCR amplification of the FRT region, generating a 277 or 391 bp fragment, respectively. On the *Left*, the position of the molecular weight markers (in bp) is indicated. (*C*) Levels of *TNS3* transcripts in MACS-enriched splenic B cells sorted from wt and TNS3-nc mice were measured by RT-qPCR and normalized against *Hprt* and *Tbp1* housekeeping genes. (*D*) Basal levels of IgM and IgG1 antibodies in the serum of nonimmunized wt and TNS3-nc mice were analyzed by ELISA. (*E–K*) Analysis of wt vs. TNS3-nc mice on day 10 after intraperitoneal immunization (Imm) with NP-CGG/alum vs. nonimmunized mice (naive), using either ELISA for serum analysis (*E* and *F*) or flow cytometry for spleen analysis (*G–K*). (*E* and *F*) NP-specific total (*E*) and high affinity (*F*) antibody titers. (*G*) Representative dot plots showing the gating of CD95^high GL7^high GC B cells among total B cells (B220⁺ CD19⁺) (*Left* graph) and the identification of NP-specific GC B cells in the two graphs on the *Right*. (*H* and *I*) Quantification of the numbers (nb) of total and NP-specific GC B cells. (*J*) Representative dot plots showing the gating strategy to identify plasma cells (PC) (CD138⁺) among total live cells (*Left* graph) and the gating for NP-specific PC. (*K*) Quantification of NP-specific PC numbers (nb). Data are from one representative experiment out of two (*D*) or a pool of five (*E* and *F*) or three (*G–K*) independent experiments, or from a single experiment (*C*). (*H*, *I*, and *K*) Due to inherent differences in the strength of the immune response between experiments, data from each experiment were normalized to the average wt levels. Bars represent means ± SEM; differences were statistically significant with $P < 0.05$ (unpaired *t* test) unless indicated otherwise (*$P < 0.05$; **$P < 0.01$; ***$P < 0.001$; n.s., not significant $P > 0.05$).

TNS3-nc would affect the T cell–dependent humoral response by immunizing wt and TNS3-nc mice intraperitonially with NP-CGG (4-Hydroxy-3-nitrophenylacetyl-chicken gamma globulin) and evaluating the splenic response 10 d later. Total IgG1 antibodies raised against NP (NP26), as well as high-affinity IgG1 antibodies to NP (NP4) were mildly reduced in the serum of TNS3-nc mice (Fig. 3 *E* and *F*). Flow cytometric analysis of the spleen for the GC response additionally revealed that both the total and NP-specific GC B cell numbers were partially decreased in TNS3-nc mice compared to their wt littermates (Fig. 3 *G–I*). The ratio of dark zone (DZ, CXCR4^{high} CD86^{low}) to light zone (LZ, CXCR4^{low} CD86^{high}) GC B cells and of total to high-affinity antibodies reactive to NP were unchanged (*SI Appendix,* Fig. S4 *E and F*), suggesting a fairly normal GC organization and function. The plasma cell (PC) compartment of the spleen was also affected in mutant mice, with NP-specific PC showing a 30% reduction compared to wt counterparts (Fig. 3 *J* and *K*). Immunization with sheep red blood cells (SRBC) led to a similar decrease in GC B cell numbers in TNS3-nc mice as with NP-CGG immunization, but without significantly affecting the PC numbers (*SI Appendix,* Fig. S4 *G and H*). Collectively, these findings suggest that Tensin-3 cleavage is largely dispensable for basal serum antibody titers and isotype switching, but contributes to the immunization-induced GC and antibody response, with more variable effects seen for early PC responses.

Tensin-3 Cleavage Leads to Reduced B Cell Adhesion. Given the limited significance of Tensin-3 cleavage for B cell responses in mice, we next focused on deciphering its role in human B cells. To understand how Tensin-3 affects processes involved in B cell activation, we monitored the effect of Tensin-3 silencing on known MALT1-dependent signaling events such as the phosphorylation of the NF-κB1 inhibitor IκB or the phosphorylation-induced activation of the Jun N-terminal kinase (JNK) pathway. Silencing of Tensin-3 in the B cell line BJAB did not affect these transcriptional responses (Fig. 4 *A* and *B*). Similarly, NF-κB1-driven luciferase activity was not affected by Tensin-3 silencing (Fig. 4*C*). In epithelial cells, Tensin-3 has been reported to control cellular adhesiveness, by binding to the cytoplasmic domain of integrin β chains and linking these adhesion receptors to the actin cytoskeleton (27, 38). To determine whether Tensin-3 plays a role in B lymphocyte adhesion, we silenced Tensin-3 in BJAB cells stimulated with PMA and ionomycin and analyzed integrin-mediated cell adhesion using plates coated with the β1 integrin ligands fibronectin and VCAM-1 or the β2 integrin ligand ICAM-1. Deletion of Tensin-3 led to a clear reduction in the stimulation-induced cellular adhesion with all three ligands (Fig. 4*D*). A similar reduction of β2 integrin-dependent adhesion to ICAM-1 was observed for SUDHL-4 cells that were silenced for Tensin-3 (Fig. 4*E*).

To study the relevance of Tensin-3 cleavage in B cell adhesion, we reconstituted Tensin-3 silenced BJAB cells with a wt or non-cleavable form of Tensin-3 (Tensin-3-nc), mutated at both cleavage sites (Fig. 4*F*). Unstimulated cells expressing Tensin-3-nc showed a basal increase in adhesion to fibronectin-coated plates, possibly because of low basal MALT1 activity in the cells (Fig. 4*G*). Compared to wt Tensin-3, cells expressing Tensin-3-nc also showed significantly increased adhesion to fibronectin or ICAM-1 upon stimulation of the cells with PMA and ionomycin (Fig. 4*G*). Similar observations were made when monitoring the fibronectin-dependent adhesion of primary splenic B cells isolated from wt or Tensin-3-nc mice (Fig. 4*H*). Stimulation of the cells with PMA and ionomycin for 30 min or 3h induced an increase in B cell adhesiveness, and B cells expressing Tensin-3-nc manifested a stronger capacity to adhere to fibronectin, which was statistically significant at both time points

(Fig. 4*H*). Collectively, these findings support a role for human and mouse Tensin-3 in integrin-dependent B cell adhesion and suggest that MALT1-dependent Tensin-3 cleavage serves to limit the adhesiveness of stimulated B cells, possibly to allow B cells to detach from a cell presenting the native antigen, once BCR signaling has been triggered.

MALT1-Catalyzed Tensin-3 Cleavage Promotes Lymphoma Dissemination. Constitutive MALT1 activity is a hallmark of specific forms of human lymphomas, including the ABC subtype of DLBCL and a fraction of MCL (mantle cell lymphoma) (30, 31, 39). Therefore, we monitored the status of Tensin-3 cleavage in a variety of human lymphoma cell lines by western blot, using an antibody directed against the CT region of Tensin-3. This antibody detected the presence of full-length and cleaved Tensin-3 in three independent ABC DLBCL cell lines (Fig. 5*A* and *SI Appendix,* Fig. S5*A*), consistent with the original MS-based findings obtained using OCI-Ly3 cells (Fig. 1 *B* and *C*). In contrast, only full-length Tensin-3 was present in the GCB DLBCL cell lines HT, BJAB, SUDHL-4, and SUDHL-6, in which MALT1 is not active (Fig. 5*A* and *SI Appendix,* Fig. S5*A*). Pretreatment of the ABC DLBCL cell lines with the MALT1 inhibitor z-LVSR-fmk (15) inhibited cleavage of the known MALT1 substrate BCL10 (23), as expected, and led to accumulation of full-length Tensin-3 and disappearance of the CT Tensin-3 cleavage fragment (Fig. 5*B*). In HBL-1 cells, an ABC DLBCL model that expressed low levels of Tensin-3, the cleavage fragment was below detection levels, but MALT1 inhibitor treatment also led to accumulation of full-length Tensin-3 (Fig. 5*B*). This suggested that MALT1-dependent Tensin-3 cleavage served to lower Tensin-3 levels in ABC DLBCL. Constitutive MALT1-dependent Tensin-3 cleavage was also detectable in a subset of MCL cell lines that are characterized by constitutive NF-κB1 activation and MALT1 activity (39) (Fig. 5*C* and *SI Appendix,* Fig. S5*B*). In contrast, Tensin-3 cleavage was not observed in MCL cell lines relying on the NF-κB2 pathway, which lack constitutive MALT1 activity (Fig. 5*C*).

Finally, we aimed to explore whether Tensin-3 cleavage affected the proliferation of ABC DLBCL cell lines in vitro and their growth and dissemination in vivo. The large size of the Tensin-3 cDNA (4.3 kb) greatly reduces the packaging efficiency of lentiviral transduction constructs. Therefore, we did not manage to stably express wt or Tensin-3-nc in ABC DLBCL cell lines which, in contrast to BJAB cells, are more difficult to transduce. For this reason, we decided to focus on Tensin-3 silencing as a surrogate readout for the cleavage-dependent reduction of total Tensin-3 protein levels (Fig. 5*B*). First, we assessed the effect of Tensin-3 silencing on cellular growth in vitro, by transducing various ABC and GCB DLBCL cell lines with two different, doxycycline-inducible shRNAs that target Tensin-3. As controls, we used a nontoxic shRNA, as well as a Myc-specific shRNA that inhibits proliferation in DLBCL models. Silencing of Myc expression induced cytotoxicity in all cell lines tested (*SI Appendix,* Fig. S5 *C, Upper*), as previously shown (40). On the contrary, silencing of Tensin-3 using two different shRNAs had no consistent effect on the growth of these cell lines in vitro (*SI Appendix,* Fig. S5 *A and B*, *Middle* and *Lower*). We also did not observe differences in the expression of known MALT1-dependent NF-κB1 targets such as Bcl-XL and FLIP nor in the expression of the AP-1 family member c-Jun in sorted Tensin-3 silenced vs. control cells (*SI Appendix,* Fig. S5*A*). Since one of the two Tensin-3 shRNAs showed some effect on cell viability for HBL-1 cells, we additionally silenced Tensin-3 in this cell line by a CRISPR/Cas9 approach. Tensin-3 silencing was efficient (Fig. 5*D*) but did not affect cell viability of HBL-1 cells, suggesting an off-target effect of one of the Tensin-3 shRNAs (*SI Appendix,* Fig. S5*D*). We reasoned
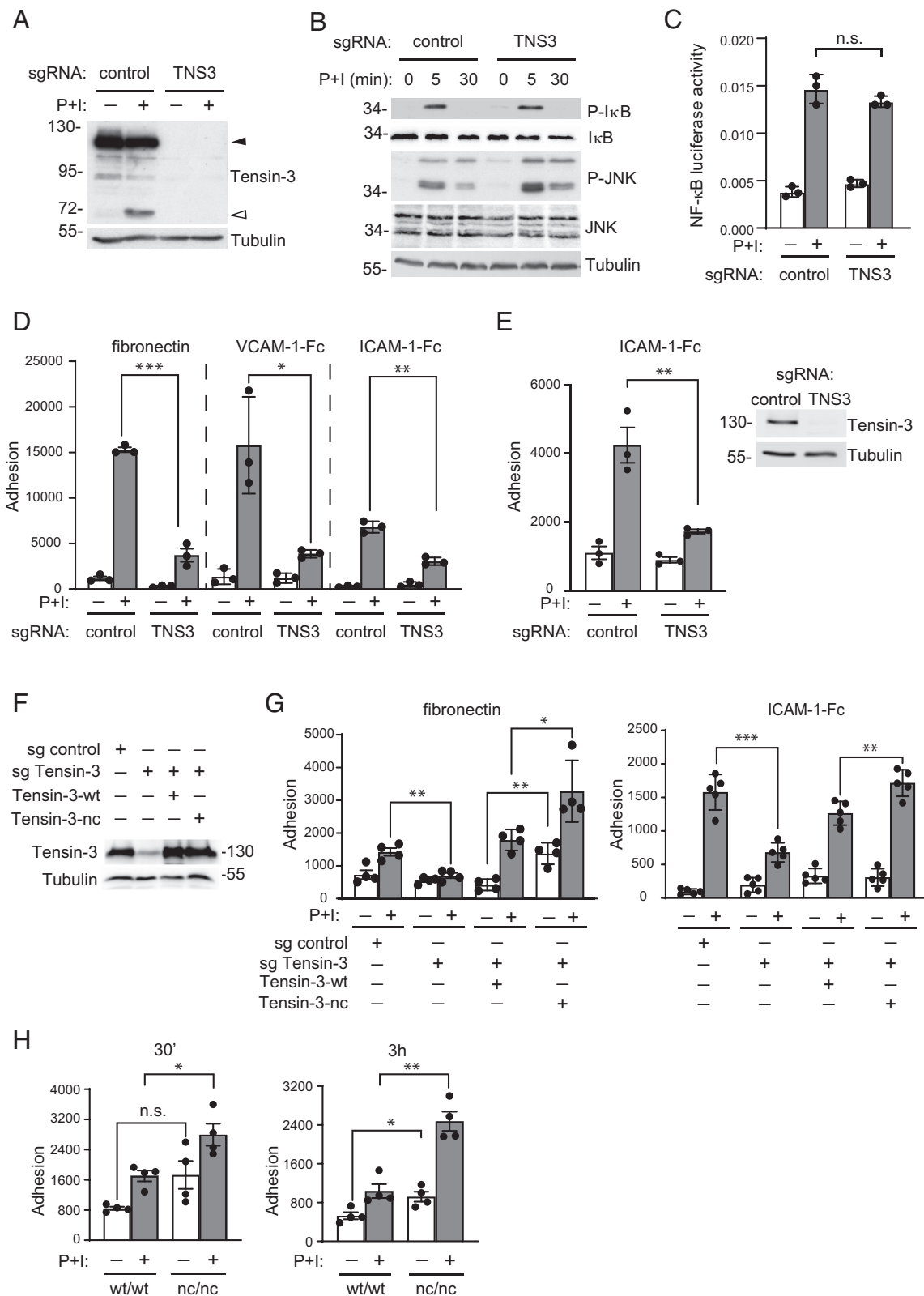
Fig. 4. Tensin-3 levels control integrin-dependent adhesion of activated B cells. (*A*) Western blot analysis of BJAB cells that were transduced with Tensin-3-specific or control CRISPR/Cas9 sgRNAs and left unstimulated or stimulated with PMA and ionomycin (P+I) for 30 min. (*B*) Western blot analysis of BJAB cells described in *A*, treated with PMA and ionomycin (P+I) or solvent alone for 5 min and 30 min, and analysed for P-IκBα, total IκBα, P-JNK, and total JNK. (*C*) NF-κB1 luciferase activity of BJAB cells from *A*, left unstimulated or stimulated with PMA and ionomycin (P+I) for 16 h. (*D*) Adhesion of unstimulated or stimulated BJAB cells from *A*, using plates coated with fibronectin, VCAM-1-Fc, or ICAM-1-Fc. (*E*) Adhesion of SUDHL-4 cells, treated with PMA and ionomycin (P+I) or solvent alone for 30 min, monitored using plates coated with ICAM-1-Fc. (*F*) Western blot analysis of BJAB cells that were transduced with Tensin-3-specific or control CRISPR/Cas9 sgRNAs and reconstituted with wt or noncleavable Tensin-3 (Tensin-3-nc) constructs, as indicated. (*G*) Adhesion of unstimulated or stimulated BJAB cells from (*F*), monitored using plates coated with fibronectin or ICAM-1-Fc. (*H*) Adhesion of murine splenic B cells expressing wildtype (wt/wt) or noncleavable Tensin-3 (nc/nc) to fibronectin-coated plates in the presence (+) or absence (−) of stimulation with PMA and ionomycin (P+I) for 30 min (*Left* panel) or 3 h (*Right* panel). Data are representative of two (*A–G*) or three (*H*) independent experiments. Bars represent means ± SEM; differences were statistically significant with $P < 0.05$ (unpaired *t* test) unless indicated otherwise (*$P < 0.05$; **$P < 0.01$; ***$P < 0.001$; n.s., not significant $P > 0.05$). Tubulin served as a loading control for western blots throughout.
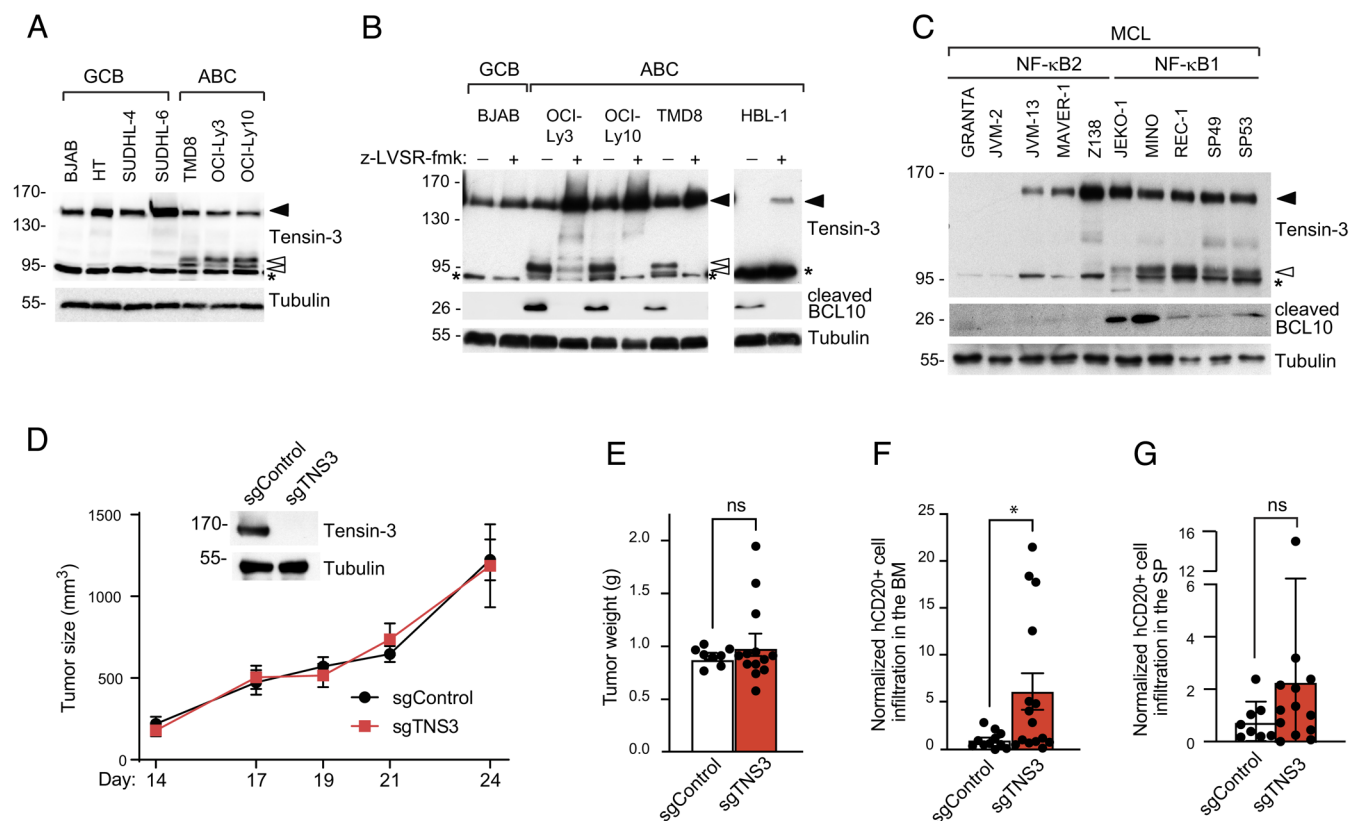
Fig. 5. Constitutive cleavage leads to decreased Tensin-3 levels, promoting dissemination of xenografted ABC DLBCL. (*A* and *B*) Immunoblot analysis of the status of Tensin-3 cleavage in lysates of the indicated GCB or ABC DLBCL cell lines (*A*), incubated for 24 h with or without z-LVSR-fmk (*B*). For the HBL-1 cell line, ten times more lysate was loaded for the Tensin-3 blot compared to the other cell lines. (*C*) Immunoblot analysis for Tensin-3 and cleaved BCL10 in lysates of MCL cell lines characterized by constitutive activation of the NF-κB2 or NF-κB1 pathway. (*D* and *E*) Tumor growth of xenografted HBL-1 cells stably transduced with control or Tensin-3-specific sgRNA (*D*) and weight of tumors excised from mice at day 24 (*E*). (*F* and *G*) Flow cytometric analysis of the presence of hCD20^{+} HBL-1 cells in the BM (*F*) or in the spleen (*G*) of NSG mice 24 d after xenografting of tumor cells into the flanks of the animals (n = 11 and 15 for control and Tensin-3 silenced cells, respectively). Data are representative of two (*A*–*D*) independent experiments. (*E*–*G*) show pooled data of 2 independent experiments. In (*F* and *G*), data were normalized to control samples. Bars represent means ± SEM; differences were statistically significant with P < 0.05 (unpaired t test) unless indicated otherwise (*P < 0.05; **P < 0.01; ***P < 0.001; n.s., not significant P > 0.05).

that even if Tensin-3 silencing did not affect cellular proliferation of lymphoma cells in vitro, it might nevertheless affect lymphomagenesis through adhesion/migration-dependent interactions with the tumor stroma and/or the neighboring cells at sites of dissemination. To test this hypothesis, we assessed the growth and dissemination of cells of the ABC DLBCL cell line HBL-1, transduced with mock or Tensin-3-targeting CRISPR/Cas9 sgRNA (single guide RNAs) constructs, upon subcutaneous xenografting into the flanks of immuno-deficient NOD scid gamma (NSG) mice. When tumor growth was monitored over time using a caliper instrument, we noticed no significant differences in tumor growth and tumor weight between the control and Tensin-3-deficient cells (Fig. 5 *D* and *E*). However, when we analyzed the BM for the presence of infiltrating hCD20^{+} tumor cells, we detected a significantly enhanced dissemination of Tensin-3 silenced cells compared to control cells. In fact, 8 out of 15 mice that received Tensin-3 silenced tumor cells showed evidence of tumor cells spreading to the BM, whereas mice that received control cells showed no or very little BM infiltration (Fig. 5*F*). The same tendency was observed when monitoring spleen infiltration (Fig. 5*G*). The fact that mice had to be put to death as soon as tumors grew to a size of 1,000 mm[3] was probably the reason why not all of them showed tumor dissemination. Together, these findings suggest that MALT1-dependent Tensin-3 cleavage, which lowers Tensin-3 levels in tumor cells, promotes the spreading of tumor cells to a distant location.

Discussion

Here, we identified the scaffold protein Tensin-3 as a MALT1 substrate and present several lines of evidence supporting a role of Tensin-3 in B cell adhesion that is negatively regulated through its MALT1-dependent cleavage. Indeed, integrin β1 and β2-dependent adhesion of B cells was impaired in cells lacking Tensin-3, whereas adhesion was enhanced in human and mouse B cells expressing a TNS3-nc as compared to a wt form. Notably, we found that suppressing Tensin-3 levels aided xenografted lymphoma cells with constitutive MALT1 activity in propagating metastatically. Collectively, these results are consistent with a scenario in which Tensin-3 cleavage by MALT1 inhibits the adhesion capacities of activated B cells and lymphoma cells.

The growing family of cellular MALT1 substrates includes BCL10 (23), RelB (14), A20 (13), HOIL-1 (19–21), CYLD (33), Regnase-1 (16), Roquin (18) and N4BP-1 (17), and MALT1 itself (15, 41). Two more proteins, the kinase NIK and the tumor suppressor LIMA1, are cleaved exclusively by the oncogenic API2-MALT1 fusion protein (24, 42). Several additional MALT1 substrates have been recently identified, whose individual roles merit further investigation (22). The majority of the MALT1 substrates that are currently identified control gene transcription during inflammatory immune responses. Tensin-3 stands out among the currently recognized MALT1 substrates for two reasons: First, it does not express in mature T cells, and second, it

specifically affects the integrin-mediated adhesiveness of B cells to control a transcription-independent element of the immune response. It is interesting to note that cleavage of two additional MALT1 substrates with known roles in transcriptional regulation has been suggested to play additional roles in cellular adhesion. TCR-induced cleavage of BCL10 promotes T cell adhesion by β1 integrins through unknown mechanisms (23), while cleavage of CYLD induces disruption of microtubules and a correlating loss of adhesiveness of vascular endothelial cells stimulated with thrombin, histamin, or lysophosphatidic acid (25). Thus, Tensin-3 is part of an emerging class of MALT1 substrates whose cleavage regulates cellular adhesiveness to control aspects of the immune response that are transcription-independent.

In the past, the role of Tensin-3 has only been investigated in nonimmune cells. Tensin-3-deficient mice have been created; these show severe growth defects and postnatal lethality, most likely resulting from defects in the development of the lung and intestinal epithelium (43). Additional studies have revealed that Tensin-3 acts as a negative regulator of cell migration and proliferation in a variety of epithelial-derived, untransformed and cancer cell lines (38, 44–46). Interestingly, Tensin-3 levels are down-regulated in tumor cells by various mechanisms, including inhibition of TNS3 gene transcription in mammary tumor cells (44) and of Tensin-3 mRNA translation in glioblastoma (46). Moreover, Tensin-3 protein function can be negatively regulated by epidermal growth factor receptor (EGFR) triggering, which induces recruitment and phosphorylation of Tensin-3, resulting in its release from focal adhesion proteins (47). The overall outcome of these processes is to down-regulate or sequester Tensin-3, thereby reducing cellular adhesion and facilitating the migration and invasive dissemination of cancer cells. Another intriguing way of regulating Tensin-3 function is through an inducible switch in expression from Tensin-3 to the Tensin homologue CTEN, whose structure closely resembles the CT Tensin-3 fragment generated by MALT1. This Tensin-3/CTEN switch, which characterizes invasive mammary tumors, has been proposed to promote cellular migration by displacing Tensin-3 from beta1 integrins, thereby disassembling fibrillar cell contacts (38, 44). In view of these findings, it is tempting to hypothesize that MALT1-dependent Tensin-3 cleavage might, at least in part, promote B cell migration and B cell lymphoma dissemination by producing a CTEN-like Tensin-3 cleavage fragment that would compete with full-length Tensin-3 for the binding to the integrin beta chain.

Triggering of the antigen receptor on B cells results in a rapid increase in integrin-mediated cellular adhesion (48–50). B cell adhesion plays an important role in the interaction of B cells with FDCs that display native antigens in the form of immune complexes (51). We propose that BCR-induced MALT1 activation, which gradually increases and peaks at about 30 min of stimulation (23), may limit the duration of B cell adhesiveness by inducing cleavage and subsequent degradation of Tensin-3, which then loosens the anchoring of beta-integrins to the cellular actin cytoskeleton (38). In our hands, activated B cells isolated from Tensin-3-nc mice showed an increase in the intensity and duration of integrin-dependent adhesiveness compared to wt B cells in vitro. This evidence did not fully translate to in vivo processes with immunized mice expressing a TNS3-nc as they displayed only a mild reduction in B cell responses, including in GC B cell numbers and antibody titers. We cannot exclude that murine B cells developing in the absence of Tensin-3 cleavage may have evolved compensatory mechanisms for these processes in vivo. It is also possible that Tensin-3 cleavage plays a stronger role in human than in murine B cells, as suggested by the more prominent defect observed for human B cells in in vitro adhesion assays, and

the ease of detecting Tensin-3 and its cleavage product in human but not murine B cells. Nevertheless, our findings point to Tensin-3 cleavage as a factor that contributes to an optimal GC B cell responses, perhaps by facilitating the detachment of naive B cells from FDCs once they have captured native antigen. The T cell–dependent humoral immune response is also impaired or delayed in mice expressing catalytically inactive MALT1 (3–6). This defect is thus likely to rely, at least in part, on MALT1-dependent Tensin-3 cleavage.

The strong constitutive cleavage of Tensin-3 that we observed in MALT1-driven lymphomas sheds light on the mechanism behind the extranodal spread of DLBCL cells with constitutive MALT1 activity. ABC subtype-typical mutations affecting *MyD88* and/or *CD79B* are more frequent in patients with multiple extranodal involvements (ENIs) compared to patients with no or single ENI (52). Among newly diagnosed patients with DLBCL, approximately 10% have BM infiltrates, and the presence of concordant BM involvement is associated with poorer outcome (53–56). When assessing the BM dissemination of xenografted ABC DLBCL HBL-1 cells, which harbor a *MyD88* and a *CD79B* mutation, we observed that Tensin-3 silencing promoted dissemination of lymphoma cells to the BM, without affecting tumor growth by itself. These findings imply that MALT1-dependent cleavage of Tensin-3 may contribute to the migration of ABC DLBCL to distant sites, possibly by promoting the detachment of tumor cells from FDCs or other cells residing in B cell follicles at the site of the primary tumor, which commonly develops at a lymph node.

Previous studies have described a role for Tensin-3 in the migration of epithelial cancer cells (44, 57). Future research into the function of Tensin-3 cleavage in solid tumors will be fascinating given the established significance of MALT1 in epithelial cancers driven by constitutive RTK and GPCR signaling (58).

In conclusion, our work identifies Tensin-3 as a substrate of MALT1-dependent cleavage in activated B cells and B cell lymphomas, with cleavage abrogating the role of Tensin-3 in integrin-mediated cell adhesion. Our research further demonstrates that loss of Tensin-3 cleavage has implications for T cell–dependent humoral immunity and that loss of Tensin-3 altogether augments human lymphoma dissemination, presumably via modulation of critical cell adhesion processes.

Materials and Methods

Identification of MALT1 Substrates by Quantitative Proteomics. The identification of MALT1 substrates by SILAC, protein separation, and quantitative MS analysis was essentially performed as described before (59, 60). Briefly, OCI-LY3 cells were cultured in modified RPMI medium containing either heavy isotope-labelled or unlabelled Lysine and Arginine for 6 passages to achieve complete labelling (>98%). Cells cultured in heavy or light medium were treated for 16 h with z- LVSR-fmk (2 μM) or solvent alone (DMSO), respectively. Cell lysates were mixed at a quantitative ratio of 1:1, and 120 μg of protein were resolved on a gradient SDS-PAGE A total of 120 μg of protein from mixed lysates was migrated on a precast 4 to 12% Novex NuPAGE Bis-Tris SDS Mini Gel (Invitrogen). After Coomassie staining, the lane was divided into 51 individual horizontal gel slices, followed by in-gel tryptic digestion and the resulting peptides in the supernatant were concentrated and analysed by liquid chromatography/tandem MS on a LTQ-Orbitrap Velos mass spectrometer (Thermo Fisher Scientific) as described (60). Protein identification in gel slices was performed with MaxQuant 1.3.0.5 (61). Proteins with different normalized SILAC ratios were visualized as a function of the gel slice using custom-made scripts as previously described (59).

Antibodies. Antibodies used in this study included polyclonal rabbit anti-hTensin-3 (C2, Santa Cruz, directed against the C terminus), affinity purified rabbit anti-hTensin-3 (generated against a GST-Tensin-3 fusion protein comprising amino acids 418 to 577 of hTensin-3), rabbit anti-BCL10 (H197, Santa Cruz Biotechnology),

anti-Tubulin, anti-FLAG (M2), anti-VSV (polyclonal and monoclonal P5D4) and anti-pERK (MAPK-YT) (Sigma), anti-pIκBα, anti-IκBα, anti-RelB, anti-JNK, anti-CARMA1, anti-Myc and anti-CYLD (Cell Signaling), anti-Strep-HRP (IBA BioTAGnology) and anti-GFP (Enzo LifeSciences). Affinity-purified MALT1 antibodies and antibodies specific for cleaved BCL10 have been previously described (23, 30). Horseradish peroxidase–coupled goat anti-mouse or anti-rabbit were from Jackson ImmunoResearch. The following antibodies were used for flow cytometry: anti-human CD20-FITC (2H7 from eBioscience); anti-mouse CD19 PE-TexasRed (1D3), B220 BV421 (RA3-6B2), CD138 BB515 (281-2), CD23 BB700 (B3 B4), CD8α APC-H7 (53-6.7) from BD Biosciences; anti-mouse CD21 PE-Cy-7 (eBioBD9), IgM APC (II/41), CD5 APC (53-73) and FoxP3 PE (FJK-16 s) from eBioscience; anti-mouse Cxcr4 PE (2811) from Invitrogen; anti-mouse CD86 FITC (GL-1), B220 AF700 (RA3-6B2), GL7 Pacific blue (GL7), CD95 PerCP Cy5.5 (SA367H8), TCRβ APC-Cy7 (H57-597), CD45 APC-Cy7 (30-F11) from BioLegend; anti-mouse CD4 PerCP (RM 4-5) from BD Pharmingen. NP-PE was purchased from Biosearch Technologies.

Cell Culture and Cell Stimulation. HEK293T cells were cultured in Dulbecco's modified Eagle's medium (DMEM) supplemented with 10% fetal calf serum (FCS) and antibiotics, respectively. Lentivirally transduced cells were always kept under puromycin selection (1 μg/mL). The diffuse large B cell lymphoma cell lines BJAB, SUDHL-4, SUDHL-6, HT, OCI-Ly1, HBL-1, OCI-Ly3, OCI-Ly10, TMD8, and U2932 and the MCL cell lines Z138, MAVER-1, JECO-1, MINO, and REC-1 (all kindly provided by Louis Staudt, NCI, Bethesda, MD, USA) were cultured as described (30, 62), and their identity was certified by genotype-based cell line authentication (Microsynth). To stimulate B and T cells, we used PMA (10 ng/mL; Alexis) and ionomycin (1 μM; Calbiochem). In some experiments, cells were preincubated with z-LVSR-fmk (2 μM, Bachem) or thioridazine (10 μM, Sigma).

Plasmids. Expression constructs for GPF-Tensin-1, GFP-Tensin-2, GFP-Tensin-3, and GFP-Tensin-4 were a kind gift from Katherine Clark (University of Leicester). The lentiCRISPRv2 vector (GeCKO) was used for CRISPR/Cas9-mediated Tensin-3 silencing. Reconstitution with Tensin-3 expression constructs was performed using a previously described retroviral vector (63). Silent point mutations and nc point mutants were generated by quick-change PCR using Kapa high-fidelity DNA polymerase (Roche), and all mutations were verified by sequencing.

Transfection and Transduction of Cells. Transient transfection of HEK293T cells and lentiviral transduction of lymphocyte cell lines were essentially performed as previously described (23). To stably silence Tensin-3 expression, BJAB and HBL-1 cells were stably transduced with two Tensin-3-specific sgRNA (5′-GTACAGTGGGACCCGCCACG-3′, 5′-GTGTACCATATGCAAGGCGC-3′) or control (luciferase-specific) sgRNA (5′-CTTCGAAATGTCCGTTCGGT-3′) and selected using puromycin. For luciferase assays, another control single guide RNA (5′-GCCCCGCCGCCCTCCCCTCC-3′) was used and selected using puromycin. Cells were subsequently transduced to constitutively express GFP together with wt or nc Tensin-3 constructs that were rendered CRISPR/Cas9 resistant by a silent point mutation. Transduced cells were sorted for live GFP-positive cells using flow cytometry. The shRNA-mediated RNA interference and cytotoxicity assays were performed as previously described (64). DLBCL cell lines were transduced with two Tensin-3 shRNA (5′-CCACTGTTTGCCATCATCTAA-3′ and 5′-GTTCTGGTACAAGGCGGATAT-3′) or a Myc shRNA (5′-CGATTCCTTCTAACAGAAATG-3′).

Cell Lysis and Immunoblotting. Cells were lysed in lysis buffer containing 50 mM 4-(2-hydroxyethyl)-1-piperazineethanesulfonic acid (HEPES) pH 7.5, 150 mM NaCl, 1% Triton-X-100, protease inhibitors (Complete; Roche), and phosphatase inhibitors (NaF, $Na_4P_2O_7$, and Na_3VO_4). Samples were boiled in reduced SDS sample buffer and subjected to SDS-PAGE and western blot as described (23).

Generation of Mice Expressing nc Tensin-3. To generate a targeting vector, an approximately 12.7-kb region of the TNS3 gene was first subcloned from a positively identified C57BL/6 fosmid clone (WI1-133G6) using a homologous recombination-based technique. The region was designed such that the 5′ homology arm extends 8.6 kb 5′ to the knock-in mutations. The 3′ homology arm extends 2.7 kb 3′ to the FRT (flippase recombinase target)-flanked Neo cassette. The FRT-flanked Neo cassette is inserted downstream of exon 17. The mutations are introduced in exon 17 with the following altering sequences: CGC>GCC for **R**614A and AGA > GCA for **R**645A. The targeting vector was confirmed by restriction analysis after each modification step and by sequencing using primers designed to read from the selection cassette into the 3′ end of the middle arm and the 5′ end of the short

arm. The knock-in mutations in exon 17 were confirmed by sequencing. The linearized targeting vector was electroporated into C57BL/6 embryonic stem cells (ES), and positive ES clones were used for injection into C57BL/6 blastocysts (inGenious Targeting Laboratory). To delete the neomycin resistance cassette in the resulting TNS3-nc-neo mice, they were bred to C57BL/6 FLP mice, and Neo deletion was confirmed by PCR. Tensin-3 knock-in and wt mice were genotyped by PCR-mediated amplification of a 391-bp or 277-bp fragment, respectively (5′- TGT GGG CCT TTC TGC CTT AAA -3′ and 5′- GTT CCG CCC ACG TCA TAC AC -3′). All mice were maintained on a C57BL/6N background in the specific pathogen-free animal facility of the University of Lausanne. Adult female mice of 8 to 12 wk of age were analyzed. All mouse experiments were authorized by the Swiss Federal Veterinary Office.

Mouse Immunization. Wt and TNS3 nc/nc littermates (8 to 12 wk old) were immunized by intraperitoneal injection with 200 μg of NP-CGG (Biosearch Technology) in alum (Thermo Fisher Scientific) or with 200 μL of SRBC (Atlantis). Serum and spleen were harvested for analysis at day 10 after immunization.

Flow Cytometry Analysis. Single-cell suspensions from half spleens and inguinal lymph nodes were prepared by gentle mechanical dissociation of respective tissues using a plunger and passage of cells through a 70-μm filter. The BM was harvested from femurs and tibias, which were cut at far end, and BM cells were harvested by centrifugation for 1 min at 13,000 rpm in culture medium (RPMI with 10% FCS). Spleen and BM cells were counted after erythrocyte lysis in ACK buffer (Gibco). Fc receptors were blocked by incubating cells in staining buffer (PBS supplemented with 2% heat-inactivated FCS) with anti-CD16/CD32 antibodies (2.4G2, hybridoma supernatant). Staining was performed in staining buffer on ice for 30 min with optimal dilutions. Intracellular staining was performed using the Cytofix/Cytoperm kit (BD Biosciences) according to the manufacturer's instruction. Viability dye (Invitrogen) was routinely used to exclude dead cells. Data were acquired on a LSR II flow cytometer (both BD Biosciences) and analysed using FlowJo software (TreeStar).

Isolation of Primary B and T Cells. Primary human B and T cells were isolated from healthy donors by magnetic affinity cell sorting (MACS) beads according to the manufacturer's description (Miltenyi MACS 130-045-101 for T cells and MACS 130-091-151 for B cells). Isolation of splenocytes and B cell purification from mice was performed using the B-cell isolation kit according to the manufacturer's description (Miltenyi MACS 130-090-862).

In Vitro Proliferation. A total of 2×10^5 splenocytes labelled with CTV (Invitrogen) were plated in 96-well round-bottom plates (COSTAR) and treated with different stimuli: CpG (3 μg/mL, 1826 Olg ID #833175 from Pascal Schneider), PMA (10 ng/mL; Alexis) and ionomycin (1 μM; Calbiochem), and IgM (10 μg/mL AffiniPure F(ab')2; Jackson ImmunoResearch). After 4 d, CTV dilution was analysed by FACS.

Quantitative Real-Time PCR. B cells from naive murine spleens were purified by MACS and lysed in TRIzol (Ambion, Life Technologies), followed by RNA extraction, RT, cDNA purification, real-time qPCR, and normalization as described previously (65). Sequences of primer pairs used are as follows: *Hprt*: Fwd: 5′- GTTGGATATGCCCTTGAC-3′ Rev: 5′-AGGACTAGAACACCTGCT-3′; *Tbp*: Fwd: 5′-CCTTCACCAATGACTCCTATGAC-3′ and Rev:5′-CAAGTTTACAGCCAAGATTCAC-3′; *TNS3*: Fwd:5′-AGAACATGAGTGCGGATGGA-3′ and Rev: 5′-CCGTGGTCTGGACTGCTAG-3′.

NF-κB1 Luciferase Assay. Activation of gene transcription was assessed by transient electroporation of control or Tensin-3-silenced cells with a NF-κB1 firefly luciferase reporter construct together with a Renilla luciferase vector (phRL-TK). Cells were lysed in passive lysis buffer (Promega), and luciferase activity was assessed using dual luciferase assay (Promega) on a TD-20/20 luminometer (Turner Design, Fisher Scientific).

Cell Viability Assay. HBL-1 control or Tensin-3 KO cells were plated at the same density (2.5×10^5/mL). One week later viability was assessed with an MTS/PMS assay, using 3-(4,5-dimethylthiazol-2-yl)-5-(3-carboxymethoxyphenyl)-2-(4-sulfophenyl)-2H-tetrazolium (MTS) (Promega, at 400 μg/mL) and phenazine methosulfate (PMS) Sigma-Aldrich, at 9 μg/mL), according to the manufacturer's instructions. Reduction of MTS to formazan was measured at 492 nm with Capture 96 Software.

Adhesion Assay. Ninety-six-well cell culture plates (Sigma) were coated O/N at 4 °C with 50 μL of fibronectin (50 μg/mL; Roche), VCAM-1-Fc (10 μg/mL; R&D System), or ICAM-Fc (50 μg/mL; R&D System). Coated wells were washed

once with PBS (without Ca2+ and Mg2+) and were blocked for 2 h with 1% BSA in PBS. A total of 10^5 cells were left unstimulated or stimulated for the indicated time at 37 °C with PMA (10 ng/mL; Alexis) and ionomycin (1 μM; Calbiochem) or solvent (DMSO). Cells were added to the coated tissue culture plates for 1 h, unless otherwise indicated. Subsequently, nonadherent cells were removed by washing of the wells three to five times with Hank's balanced salt solution. Adherent cells were counted using Spectramax (Molecular Devices) and quantified with ImageJ.

Detection of Serum Antibodies by ELISA. For NP-specific antibody detection, Nunc Immuno Plate MaxiSorp plates (Thermo Fisher Scientific) were coated either with 50 μg/mL NP4-BSA or 50 μg/mL NP26-BSA and incubated overnight at 4 °C. After blocking with 2% BSA in PBS, the plates were incubated with serially diluted serum samples and then with biotin-conjugated detection antibodies (Southern Biotech) followed by streptavidin-conjugated HRP (Jackson ImmunoResearch). After colorimetric reaction (SigmaFAST OPD tablets), the absorbance at 490 nm was measured using an enzyme-linked immunosorbent assay (ELISA) plate reader. Serum dilutions giving OD50 values for wt sera were chosen. For total Ig detection, Nunc Immuno Plate MaxiSorp plates were coated with 5 μg/mL anti–Ig capture antibody (Southern Biotech) and incubated overnight at 4 °C. After blocking with 2% BSA in PBS, the plates were incubated with serially diluted serum samples, detected with isotype-specific antibodies (SouthernBiotech), and developed as described above.

Xenograft Experiments. NSG mice were maintained under pathogen-free conditions in the animal facility of the University of Lausanne. For xenograft studies, NSG mice were inoculated with 10^5 HBL-1 cells expressing different sgRNAs, mixed with Matrigel (Corning) and PBS in a 1:1 ratio, into the flanks of the animals. Tumor volume was determined by digital caliper measurements and calculated by using the formula (length × width squared)/2. Tumor weight was determined at day 24, when mice were killed. Spreading to the BM and spleen was assessed by measuring the percentage of hCD20+ cells.

Statistical Analysis. For statistical analysis, prism software was used, and two-tailed Student's *t* test was applied; *P* values ≤0.05 were considered statistically significant.

Data, Materials, and Software Availability. All study data are included in the article and/or supporting information.

Author affiliations: [a]Department of Immunobiology, University of Lausanne, Epalinges CH-1066, Switzerland; and [b]Department of Medicine A for Hematology, Oncology and Pneumology, University Hospital Münster, Münster D-48149, Germany

1. I. Meininger, D. Krappmann, Lymphocyte signaling and activation by the CARMA1-BCL10-MALT1 signalosome. *Biol. Chem.* **397**, 1315–1333 (2016).
2. J. Ruland, L. Hartjes, CARD-BCL-10-MALT1 signalling in protective and pathological immunity. *Nat. Rev. Immunol.* **19**, 118–134 (2019).
3. M. Jaworski *et al.*, Malt1 protease inactivation efficiently dampens immune responses but causes spontaneous autoimmunity. *EMBO J.* **33**, 2765–2781 (2014).
4. A. Gewies *et al.*, Uncoupling Malt1 threshold function from paracaspase activity results in destructive autoimmune inflammation. *Cell Rep.* **9**, 1292–1305 (2014).
5. F. Bornancin *et al.*, Deficiency of MALT1 paracaspase activity results in unbalanced regulatory and effector T and B cell responses leading to multiorgan inflammation. *J. Immunol.* **194**, 3723–3734 (2015).
6. J. W. Yu *et al.*, MALT1 protease activity is required for innate and adaptive immune responses. *PLoS One* **10**, e0127083 (2015).
7. L. Sun, L. Deng, C. K. Ea, Z. P. Xia, Z. J. Chen, The TRAF6 ubiquitin ligase and TAK1 kinase mediate IKK activation by BCL10 and MALT1 in T lymphocytes. *Mol. Cell* **14**, 289–301 (2004).
8. Q. Qiao *et al.*, Structural architecture of the CARMA1/Bcl10/MALT1 signalosome: Nucleation-induced filamentous assembly. *Mol. Cell* **51**, 766–779 (2013).
9. F. Schlauderer *et al.*, Molecular architecture and regulation of BCL10-MALT1 filaments. *Nat. Commun.* **9**, 4041 (2018).
10. C. Pelzer *et al.*, The protease activity of the paracaspase MALT1 is controlled by monoubiquitination. *Nat. Immunol.* **14**, 337–345 (2013).
11. R. Schairer *et al.*, Allosteric activation of MALT1 by its ubiquitin-binding Ig3 domain. *Proc. Natl. Acad. Sci. U.S.A.* **117**, 3093–3102 (2020).
12. H. Noels *et al.*, A Novel TRAF6 binding site in MALT1 defines distinct mechanisms of NF-kappaB activation by API2middle dotMALT1 fusions. *J. Biol. Chem.* **282**, 10180–10189 (2007).
13. B. Coornaert *et al.*, T cell antigen receptor stimulation induces MALT1 paracaspase-mediated cleavage of the NF-kappaB inhibitor A20. *Nat. Immunol.* **9**, 263–271 (2008).
14. S. Hailfinger *et al.*, Malt1-dependent RelB cleavage promotes canonical NF-kappaB activation in lymphocytes and lymphoma cell lines. *Proc. Natl. Acad. Sci. U.S.A.* **108**, 14596–14601 (2011).
15. M. Baens *et al.*, MALT1 auto-proteolysis is essential for NF-kappaB-dependent gene transcription in activated lymphocytes. *PLoS One* **9**, e103774 (2014).
16. T. Uehata *et al.*, Malt1-induced cleavage of regnase-1 in CD4(+) helper T cells regulates immune activation. *Cell* **153**, 1036–1049 (2013).
17. D. Yamasoba *et al.*, N4BP1 restricts HIV-1 and its inactivation by MALT1 promotes viral reactivation. *Nat. Microbiol.* **4**, 1532–1544 (2019).
18. K. M. Jeltsch *et al.*, Cleavage of roquin and regnase-1 by the paracaspase MALT1 releases their cooperatively repressed targets to promote T(H)17 differentiation. *Nat. Immunol.* **15**, 1079–1089 (2014).
19. T. Klein *et al.*, The paracaspase MALT1 cleaves HOIL1 reducing linear ubiquitination by LUBAC to dampen lymphocyte NF-kappaB signalling. *Nat. Commun.* **6**, 8777 (2015).
20. T. Douanne, J. Gavard, N. Bidere, The paracaspase MALT1 cleaves the LUBAC subunit HOIL1 during antigen receptor signaling. *J. Cell Sci.* **129**, 1775–1780 (2016).
21. L. Elton *et al.*, MALT1 cleaves the E3 ubiquitin ligase HOIL-1 in activated T cells, generating a dominant negative inhibitor of LUBAC-induced NF-kappaB signaling. *FEBS J.* **283**, 403–412 (2016).
22. P. A. Bell *et al.*, Integrating knowledge of protein sequence with protein function for the prediction and validation of new MALT1 substrates. *Comput. Struct. Biotechnol. J.* **20**, 4717–4732 (2022).
23. F. Rebeaud *et al.*, The proteolytic activity of the paracaspase MALT1 is key in T cell activation. *Nat. Immunol.* **9**, 272–281 (2008).
24. Z. Nie *et al.*, Conversion of the LIMA1 tumour suppressor into an oncogenic LMO-like protein by API2-MALT1 in MALT lymphoma. *Nat. Commun.* **6**, 5908 (2015).
25. L. R. Klei *et al.*, MALT1 protease activation triggers acute disruption of endothelial barrier integrity via CYLD cleavage. *Cell Rep.* **17**, 221–232 (2016).
26. S. H. Lo, Tensin. *Int. J. Biochem. Cell Biol.* **36**, 31–34 (2004).
27. A. Blangy, Tensins are versatile regulators of Rho GTPase signalling and cell adhesion. *Biol. Cell* **109**, 115–126 (2017).
28. T. Trub *et al.*, Specificity of the PTB domain of Shc for beta turn-forming pentapeptide motifs amino-terminal to phosphotyrosine. *J. Biol. Chem.* **270**, 18205–18208 (1995).
29. D. A. Calderwood *et al.*, Integrin beta cytoplasmic domain interactions with phosphotyrosine-binding domains: A structural prototype for diversity in integrin signaling. *Proc. Natl. Acad. Sci. U.S.A.* **100**, 2272–2277 (2003).
30. S. Hailfinger *et al.*, Essential role of MALT1 protease activity in activated B cell-like diffuse large B-cell lymphoma. *Proc. Natl. Acad. Sci. U.S.A.* **106**, 19946–19951 (2009).
31. U. Ferch *et al.*, Inhibition of MALT1 protease activity is selectively toxic for activated B cell-like diffuse large B cell lymphoma cells. *J. Exp. Med.* **206**, 2313–2320 (2009).
32. D. Nagel *et al.*, Pharmacologic inhibition of MALT1 protease by phenothiazines as a therapeutic approach for the treatment of aggressive ABC-DLBCL. *Cancer Cell* **22**, 825–837 (2012).
33. J. Staal *et al.*, T-cell receptor-induced JNK activation requires proteolytic inactivation of CYLD by MALT1. *EMBO J.* **30**, 1742–1752 (2011).
34. J. Hachmann *et al.*, Mechanism and specificity of the human paracaspase MALT1. *Biochem. J.* **443**, 287–295 (2012).
35. M. Juilland, M. Thome, Holding All the CARDs: How MALT1 Controls CARMA/CARD-Dependent Signaling. *Front. Immunol.* **9**, 1927 (2018).
36. J. Ruland, G. S. Duncan, A. Wakeham, T. W. Mak, Differential requirement for Malt1 in T and B cell antigen receptor signaling. *Immunity* **19**, 749–758 (2003).
37. A. A. Ruefli-Brasse, D. M. French, V. M. Dixit, Regulation of NF-kappaB-dependent lymphocyte activation and development by paracaspase. *Science* **302**, 1581–1584 (2003).
38. Y. Pylayeva, F. G. Giancotti, Tensin relief facilitates migration. *Nat. Cell Biol.* **9**, 877–879 (2007).
39. R. Rahal *et al.*, Pharmacological and genomic profiling identifies NF-kappaB-targeted treatment strategies for mantle cell lymphoma. *Nat. Med.* **20**, 87–92 (2014).
40. B. Dai *et al.*, B-cell receptor-driven MALT1 activity regulates MYC signaling in mantle cell lymphoma. *Blood* **129**, 333–346 (2017).
41. C. H. Wu *et al.*, Autocleavage of the paracaspase MALT1 at Arg-781 attenuates NF-kappaB signaling and regulates the growth of activated B-cell like diffuse B-cell lymphoma cells. *PLoS One* **13**, e0199779 (2018).
42. S. Rosebeck *et al.*, Cleavage of NIK by the API2-MALT1 fusion oncoprotein leads to noncanonical NF-kappaB activation. *Science* **331**, 468–472 (2011).
43. M. K. Chiang, Y. C. Liao, Y. Kuwabara, S. H. Lo, Inactivation of tensin3 in mice results in growth retardation and postnatal lethality. *Dev. Biol.* **279**, 368–377 (2005).
44. M. Katz *et al.*, A reciprocal tensin-3-cten switch mediates EGF-driven mammary cell migration. *Nat. Cell Biol.* **9**, 961–969 (2007).
45. D. Martuszewska *et al.*, Tensin3 is a negative regulator of cell migration and all four Tensin family members are downregulated in human kidney cancer. *PLoS One* **4**, e4350 (2009).
46. H. Y. Chen *et al.*, Musashi-1 enhances glioblastoma cell migration and cytoskeletal dynamics through translational inhibition of Tensin3. *Sci. Rep.* **7**, 8710 (2017).
47. Y. Cui, Y. C. Liao, S. H. Lo, Epidermal growth factor modulates tyrosine phosphorylation of a novel tensin family member, tensin3. *Mol. Cancer Res.* **2**, 225–232 (2004).

48. L. H. Dang, K. L. Rock, Stimulation of B lymphocytes through surface Ig receptors induces LFA-1 and ICAM-1-dependent adhesion. *J. Immunol.* **146**, 3273–3279 (1991).

49. G. Koopman *et al.*, Adhesion of human B cells to follicular dendritic cells involves both the lymphocyte function-associated antigen 1/intercellular adhesion molecule 1 and very late antigen 4/vascular cell adhesion molecule 1 pathways. *J. Exp. Med.* **173**, 1297–1304 (1991).

50. M. Spaargaren *et al.*, The B cell antigen receptor controls integrin activity through Btk and PLCgamma2. *J. Exp. Med.* **198**, 1539–1550 (2003).

51. M. H. Kosco-Vilbois, Are follicular dendritic cells really good for nothing? *Nat. Rev. Immunol.* **3**, 764–769 (2003).

52. R. Shen *et al.*, Influence of oncogenic mutations and tumor microenvironment alterations on extranodal invasion in diffuse large B-cell lymphoma. *Clin. Transl. Med.* **10**, e221 (2020).

53. J. Campbell *et al.*, The prognostic impact of bone marrow involvement in patients with diffuse large cell lymphoma varies according to the degree of infiltration and presence of discordant marrow involvement. *Eur. J. Haematol.* **76**, 473–480 (2006).

54. R. Chung *et al.*, Concordant but not discordant bone marrow involvement in diffuse large B-cell lymphoma predicts a poor clinical outcome independent of the International Prognostic Index. *Blood* **110**, 1278–1282 (2007).

55. L. H. Sehn *et al.*, Impact of concordant and discordant bone marrow involvement on outcome in diffuse large B-cell lymphoma treated with R-CHOP. *J. Clin. Oncol.* **29**, 1452–1457 (2011).

56. D. Muringampurath-John *et al.*, Characteristics and outcomes of diffuse large B-cell lymphoma presenting in leukaemic phase. *Br. J. Haematol.* **158**, 608–614 (2012).

57. X. Qian *et al.*, The Tensin-3 protein, including its SH2 domain, is phosphorylated by Src and contributes to tumorigenesis and metastasis. *Cancer Cell* **16**, 246–258 (2009).

58. B. Gomez Solsona, A. Schmitt, K. Schulze-Osthoff, S. Hailfinger, The Paracaspase MALT1 in Cancer. *Biomedicines* **10**, 344 (2022).

59. A. Di Micco *et al.*, AIM2 inflammasome is activated by pharmacological disruption of nuclear envelope integrity. *Proc. Natl. Acad. Sci. U.S.A.* **113**, E4671–E4680 (2016).

60. K. Morikawa *et al.*, Quantitative proteomics identifies the membrane-associated peroxidase GPx8 as a cellular substrate of the hepatitis C virus NS3-4A protease. *Hepatology* **59**, 423–433 (2014).

61. J. Cox, M. Mann, MaxQuant enables high peptide identification rates, individualized p.p.b.-range mass accuracies and proteome-wide protein quantification. *Nat. Biotechnol.* **26**, 1367–1372 (2008).

62. M. Juilland *et al.*, CARMA1- and MyD88-dependent activation of Jun/ATF-type AP-1 complexes is a hallmark of ABC diffuse large B-cell lymphomas. *Blood* **127**, 1780–1789 (2016).

63. J. W. Neal, N. A. Clipstone, Calcineurin mediates the calcium-dependent inhibition of adipocyte differentiation in 3T3-L1 cells. *J. Biol. Chem.* **277**, 49776–49781 (2002).

64. H. Nogai *et al.*, IkappaB-zeta controls the constitutive NF-kappaB target gene network and survival of ABC DLBCL. *Blood* **122**, 2242–2250 (2013).

65. A. Link *et al.*, Fibroblastic reticular cells in lymph nodes regulate the homeostasis of naive T cells. *Nat. Immunol.* **8**, 1255–1265 (2007).